Article

Neuron

Peri-Synaptic Glia Recycles Brain-Derived Neurotrophic Factor for LTP Stabilization and Memory Retention

Highlights

- Peri-synaptic glia provides proBDNF clearing and recycling via $p75^{NTR}$ receptor
- Glial BDNF recycling results in localized TrkB phosphorylation on adjacent neurons
- Glial BDNF recycling is relevant for LTP maintenance at cortical synapses
- Mice deficient in BDNF glial recycling fail to recognize familiar from novel objects

Authors

Beatrice Vignoli, Giulia Battistini, Riccardo Melani, Robert Blum, Spartaco Santi, Nicoletta Berardi, Marco Canossa

Correspondence

beatrice.vignoli@unitn.it (B.V.), marco.canossa@unitn.it (M.C.)

In Brief

Vignoli et al. identified a novel mechanism by which peri-synaptic glia provides proBDNF clearing and recycling, a process that is required for sustaining LTP. Impairment in BDNF glial recycling in vivo leads to malfunctions in cortical synapses and behavior.

Vignoli et al., 2016, Neuron *92*, 873–887
November 23, 2016
http://dx.doi.org/10.1016/j.neuron.2016.09.031

CellPress

Neuron
Article

Peri-Synaptic Glia Recycles Brain-Derived Neurotrophic Factor for LTP Stabilization and Memory Retention

Beatrice Vignoli,[1,7,*] Giulia Battistini,[2] Riccardo Melani,[3] Robert Blum,[4] Spartaco Santi,[5] Nicoletta Berardi,[3,6] and Marco Canossa[1,7,8,*]
[1]European Brain Research Institute (EBRI) "Rita Levi-Montalcini", via del Fosso di Fiorano 64, 00143 Rome, Italy
[2]Department of Pharmacy and Biotechnology (FaBiT), University of Bologna, via San Donato 15, 40127 Bologna, Italy
[3]National Research Council (CNR), Institute of Neuroscience, via Moruzzi 1, 56100 Pisa, Italy
[4]Institute for Clinical Neurobiology, University Hospital, Julius Maximilians University, Versbacher Straße 5, 97078 Würzburg, Germany
[5]National Research Council (CNR), Institute of Molecular Genetics (IGM), Laboratory of Muscoloskeletal Cell Biology, IOR, via di Barbiano1/10, 40136 Bologna, Italy
[6]Department of Neuroscience, Psychology, Drug Research, and Child Health (NEUROFARBA), University of Florence, via di San Salvi 26, 50100 Florence, Italy
[7]Centre for Integrative Biology (CIBIO), University of Trento, via Sommarive 9, 38123 Povo (TN), Italy
[8]Lead Contact
*Correspondence: beatrice.vignoli@unitn.it (B.V.), marco.canossa@unitn.it (M.C.)
http://dx.doi.org/10.1016/j.neuron.2016.09.031

SUMMARY

Glial cells respond to neuronal activation and release neuroactive molecules (termed "gliotransmitters") that can affect synaptic activity and modulate plasticity. In this study, we used molecular genetic tools, ultra-structural microscopy, and electrophysiology to assess the role of brain-derived neurotrophic factor (BDNF) on cortical gliotransmission in vivo. We find that glial cells recycle BDNF that was previously secreted by neurons as pro-neurotrophin following long-term potentiation (LTP)-inducing electrical stimulation. Upon BDNF glial recycling, we observed tight, temporal, highly localized TrkB phosphorylation on adjacent neurons, a process required to sustain LTP. Engagement of BDNF recycling by astrocytes represents a novel mechanism by which cortical synapses can expand BDNF action and provide synaptic changes that are relevant for the acquisition of new memories. Accordingly, mice deficient in BDNF glial recycling fail to recognize familiar from novel objects, indicating a physiological requirement for this process in memory consolidation.

INTRODUCTION

Brain-derived neurotrophic factor (BDNF), the most abundant neurotrophin in the brain, is primarily produced by neurons, and BDNF levels are rapidly and strongly regulated by neuronal activity (Edelmann et al., 2014; Lessmann and Brigadski, 2009; Park and Poo, 2013). In particular, synaptic modifications induced by defined activity patterns, such as theta-burst stimulation (TBS), are associated with an increase in BDNF synthesis at both transcriptional and translational levels and in BDNF secretion, which regulate fine spatial-temporal availability of the neurotrophin. It has been proposed that BDNF actions depend upon it being released as precursor (proBDNF) or as mature BDNF protein, as these two different neurotrophin isoforms exhibit opposite effects on synaptic strength (Hempstead, 2015; Lu et al., 2005; Teng et al., 2010). Mature BDNF facilitates hippocampal long-term potentiation (LTP) through TrkB receptors (Figurov et al., 1996; Korte et al., 1996; Patterson et al., 1996), whereas proBDNF facilitates hippocampal long-term depression (LTD) by activating the pan-neurotrophin receptor p75 ($p75^{NTR}$) (Lu et al., 2005; Rösch et al., 2005; Woo et al., 2005; Yang et al., 2014). Following secretion, cleavage of proBDNF by tissue plasminogen activator (tPa)/plasmin in the extracellular milieu (Pang et al., 2004) can also occur, leading to mature BDNF release and LTP maintenance. These properties suggest that expression and secretion of the different BDNF isoforms is highly regulated and proBDNF processing at synaptic sites can control plasticity (Greenberg et al., 2009).

In the present work, we have moved away from the typical target of activity-dependent BDNF secretion (neurons) and have instead investigated the role of glial cells in regulating synaptic trafficking of the neurotrophin following LTP-inducing electrical stimulation. Remarkably, we found that peri-synaptic glia uses $p75^{NTR}$ to clear proBDNF secreted from neurons and responds to neuronal activation by re-secreting proBDNF as mature neurotrophin. As a consequence of BDNF glial recycling, we observed sustained activation of TrkB on adjacent neurons required for LTP maintenance. A central hypothesis arising from this recycling pathway is that BDNF actively participates in gliotransmission and astrocytes can contribute to synaptic plasticity by modulating BDNF availability in tune with synaptic needs. Indeed, glial cells are integral to the chemical synapse, contribute to structural and functional synaptic plasticity, and play a role in the formation of new memories (Allen and Barres,

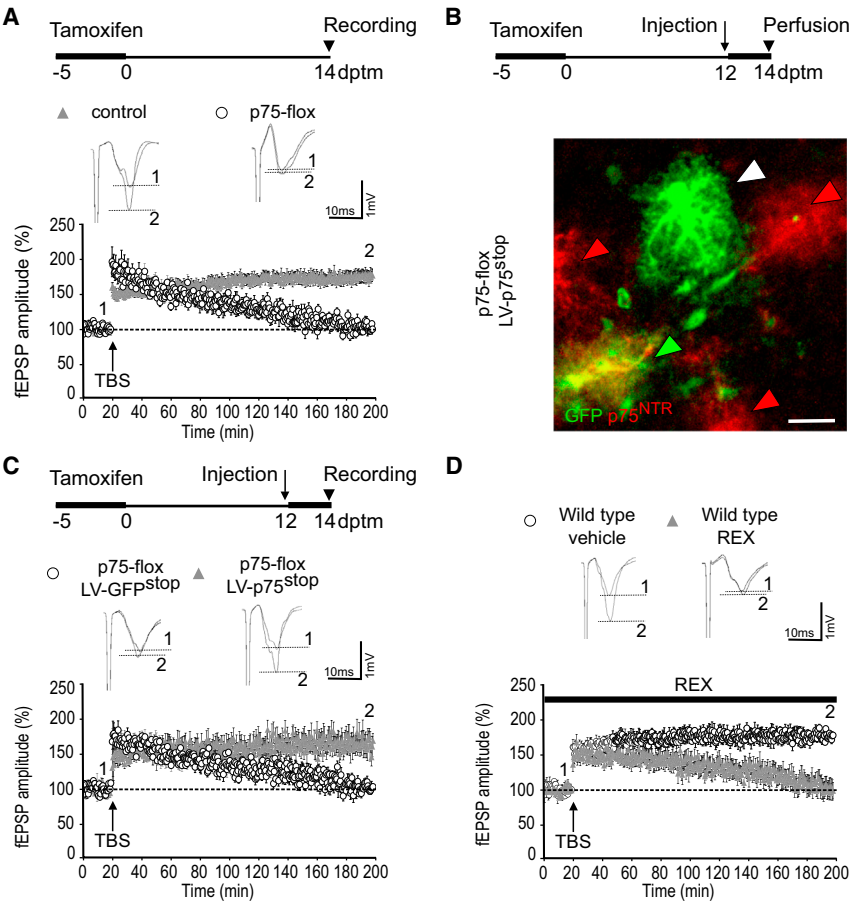

Figure 1. Glial p75^{NTR} Is Essential for LTP Maintenance

(A) Schematic diagram shows the experimental paradigm used for tamoxifen treatment in p75-flox mice and control littermates. Tamoxifen was given for 5 consecutive days (−5 to 0) and recording was performed 14 dptm. The histogram depicts LTP evoked in slices from p75-flox or control mice. Each point in the graph shows the average fEPSP amplitude elicited in response to a test stimulus before (0–20 min) and after (20–200 min) TBS stimulation. Representative fEPSP traces recorded 10 min before (1) and 180 min after (2) TBS are shown on the top (control, 164.76% ± 6.27% and p75-flox, 143.73% ± 8.81% fEPSP 60 min from TBS; control, 176.72% ± 8.67% and p75-flox, 100.58% ± 6.86% fEPSP 180 min from TBS; data are mean ± SEM; control, n = 36 slices, 27 mice; p75-flox, n = 30 slices, 20 mice; unpaired t test, $p < 0.0001$).

(B) Schematic diagram shows the experimental paradigm used for tamoxifen treatment in p75-flox mice injected with LV-p75^{stop} or LV-GFP^{stop} viruses. Following the first tamoxifen treatment (−5 to 0 days), a second treatment was applied for 2 additional days (12–14 days) after injecting the mice with lentiviral particles. The confocal image depicts non-recombined cell (white arrowhead) expressing GFP, partial-recombined cell (green arrowhead) concurrently expressing p75^{NTR} and GFP, and fully recombined cells (red arrowheads) uniquely expressing p75^{NTR}. For lentivirus description, see Figure S3A. The scale bar represents 50 μm.

(C) Schematic diagram shows the experimental paradigm as in (B); mice were injected with LV-GFP^{stop} in one hemisphere and LV-p75^{stop} in the second hemisphere. The histogram depicts LTP evoked as in (A) (LV-GFP^{stop}, 104.00% ± 3.24% and LV-p75^{stop}, 169.25% ± 10.23% fEPSP 180 min from TBS; data are mean ± SEM; LV-GFP^{stop}, n = 7 slices, 7 mice; LV-p75^{stop}, n = 8 slices, 7 mice; unpaired t test, $p < 0.0001$).

(D) Histogram depicts LTP evoked in slices from wild-type mice in the absence (vehicle) or presence (REX) of function-blocking p75^{NTR} antibody before, during, and after TBS (wild-type vehicle, 178.03% ± 11.83% and wild-type REX, 99.61% ± 3.73% fEPSP 180 min from TBS; data are mean ± SEM; REX, n = 7 slices, 4 mice; vehicle, n = 12 slices, 6 mice; unpaired t test, $p < 0.0001$).

2005; Araque et al., 2014; Halassa and Haydon, 2010), but the actual role of gliotransmission is still a matter of debate (Sloan and Barres, 2014).

In accord with the physiological properties of glial cells, we showed that BDNF glial recycling in the perirhinal cortex plays a major role in modulating cognitive behavior as visual recognition memory. Our results uncover a previously unsuspected role of cortical glial cells in regulating BDNF availability at synaptic contacts critically affecting long-term plasticity and memory consolidation.

RESULTS

Glial p75^{NTR} Is Essential for LTP Maintenance

We used tamoxifen-inducible conditional p75$^{lox/lox}$-GLAST-CreER^{T2}-R26R mutant mice (Zuccaro et al., 2014) (for simplicity, p75-flox mice) to selectively delete glial p75^{NTR} (Figures S1A–S1C, available online), the carrier receptor for proBDNF uptake by astrocytes (Bergami et al., 2008). We then observed the effects of glial p75^{NTR} deletion on LTP in cortical slices from p75-flox mice and control littermates 14 days post-tamoxifen (dptm). This timing allows for a reliable depletion of p75^{NTR} levels following Cre recombination in glial cells (Figure S1D). LTP was induced applying TBS (100 Hz; four sets of stimulations delivered 15 s apart, each one consisting of ten bursts of five pulses at 100 Hz with inter-burst intervals of 150 ms) in layer II/III of perirhinal cortices. LTP induction and maintenance were analyzed at 60 and 180 min after stimulus, respectively. In slices from control mice, TBS induced an increase in field excitatory postsynaptic potential (fEPSP) amplitude (Figure 1A) and slope (Figure S2A) that remained potentiated above baseline for the 3 hr duration of the recording. In marked contrast, TBS in slices from p75-flox mice induced only a short-lived potentiation that declined to baseline about 140 min after stimulation. Thus, glial deletion of p75^{NTR} affected the late-phase LTP. When TBS was applied in slices from p75-flox mice not induced with tamoxifen (Figure S1E), or 3 and 7 dptm before astrocytes exhibit metabolic depletion of pre-existing p75^{NTR} (Figure S1F), no deficit in

the late-phase LTP was observed, indicating that levels of $p75^{NTR}$ expression in glial cells are critical to sustain synaptic potentiation.

To firmly assess the requirement of glial $p75^{NTR}$ for LTP maintenance, we performed rescue experiments by re-expressing $p75^{NTR}$ specifically in cortical astrocytes of p75-flox mice. We engineered a lentiviral construct (LV-$p75^{stop}$) for conditional $p75^{NTR}$ expression under the control of the cytomegalovirus promoter (CMV) (Figures S3A and S3B). In this construct, a loxP-eGFP-STOP-loxP cassette allows for GFP expression, while preventing $p75^{NTR}$ expression. The eGFP-STOP cassette is removed in the presence of Cre recombinase, resulting in loss of the GFP and activation of the $p75^{NTR}$ transgene. We injected the lentiviral particles into perirhinal cortices of p75-flox mice at 12 dptm (Figure 1B). Treating mice with tamoxifen for 2 additional days after injection ensures the expression of $p75^{NTR}$ in recombined astrocytes. In parallel, slices from injected mice were used for field recordings by placing the electrodes within the area of infection. Remarkably, rescuing $p75^{NTR}$ expression in glial cells of p75-flox mice by lentiviral expression completely restores the late-phase LTP deficit (Figures 1C and S2B). Injection of a control virus (LV-GFP^{stop}) into the contralateral hemisphere of the same mice did not produce a similar effect. Here, fEPSPs declined back to baseline within 140 min after TBS. Overall, our results indicate that astroglial $p75^{NTR}$ is essential for LTP maintenance.

Next, we asked whether $p75^{NTR}$ requires endogenous neurotrophin action to sustain LTP. We used a $p75^{NTR}$ function-blocking antibody (REX) (Mischel et al., 2001) known to prevent the binding of neurotrophins to $p75^{NTR}$. Slices from wild-type mice were treated with REX (50 mg/mL) before and throughout the recording time (Woo et al., 2005). Consistent with a neurotrophin-mediated effect, perfusion with the REX antibody resulted in a short-term potentiation that declined within 140 min following stimulation (Figures 1D and S2C). In contrast, vehicle-treated slices of wild-type mice show normal LTP. These results indicate a selective role of $p75^{NTR}$ in the neurotrophin-dependent form of LTP.

Glial $p75^{NTR}$ Is Dispensable for LTD

Induction of LTD in the hippocampus requires $p75^{NTR}$ expression (Rösch et al., 2005; Woo et al., 2005), but whether glial $p75^{NTR}$ is implicated in this form of synaptic plasticity is not known. To address this issue, we monitored LTD by applying a prolonged train (10 min) of low-frequency stimulations (LFSs; 5 Hz, 3,000 pulses) to cortical slices from p75-flox mice and control littermates (Figures 2A, S2D, and S2E). LFS induced an initial decrease in fEPSP amplitude that persisted for the 180 min recording time in both genotypes. Conversely, slices perfused with REX antibody showed a decrease in fEPSP that rapidly recovered back to baseline. Thus, our data confirm the requirement of $p75^{NTR}$ in cortical LTD, but clearly indicate that glial expression of the receptor is dispensable for both LTD induction and maintenance.

ProBDNF binds and activates the $p75^{NTR}$ receptor (Teng et al., 2005) facilitating LTD induction (Woo et al., 2005; Yang et al., 2014). To determine if glial $p75^{NTR}$ mediates LTD facilitation elicited by proBDNF, the effects of a mutated form of proBDNF resistant to proteolysis ($proBDNF^{CR}$) were evaluated in cortical slices using a shorter LFS (5 Hz, 1,950 pulses, 6.5 min) (Figures 2B, S2F, and S2G). This weak stimulation did not induce LTD in vehicle-treated slices; in contrast, perfusion of $proBDNF^{CR}$ significantly enhanced LTD in slices from p75-flox mice and control littermates. Hence, $proBDNF^{CR}$ is facilitating LTD by binding to $p75^{NTR}$ receptors other than from the glial compartment.

Localization of proBDNF at Peri-Synaptic Glia

We speculated that requirement of glial $p75^{NTR}$ in LTP may be linked to its ability to promote proBDNF uptake (Bergami et al., 2008), supplying glial cells with a releasable source of the neurotrophin and enabling LTP. This implies that proBDNF is transferred from neurons to astrocytes in response to TBS, where it remains localized in vesicular structures proximal to the synapse. We investigated this scenario at light microscopic and ultra-structural levels.

To determine the intracellular localization of proBDNF in astrocytes, we performed immunostaining in cortical slices by using specific antibodies (Figure S4) selectively recognizing the precursor (α-proBDNF) or both precursor and mature forms (α-BDNF) of the neurotrophin (Figure 3A). Slices were prepared from mice previously injected with a lentivirus transducing GFP in glial cells. GFP is a cytosolic protein whose fluorescence defines the astrocyte in its entire cytoplasmic extension, a feature that is ideal for co-localization analysis. Confocal imaging and 3D reconstruction detected co-localization of proBDNF and GFP immunoreactivity (proBDNF/GFP), revealing the presence of low levels of proBDNF in single astrocytes from non-stimulated control slices (Figure 3C). Co-localization increased 10 min after TBS. This timing was chosen as it correlates with the duration of endogenous BDNF secretion that is required for LTP maintenance in this cortical area (Aicardi et al., 2004). In line with proBDNF being transferred from neurons to astrocytes, we found that proBDNF is high in the periphery of glial cells and concentrated at the margins of neuron-astrocyte contacts. Co-localization using an α-BDNF antibody showed a similar expression pattern (Figure S5). In contrast, astrocytes from p75-flox mice showed very low, if any, proBDNF/GFP co-localization (Figure 3C). A final quantitative analysis revealed that proBDNF/GFP co-localization levels increased in stimulated versus non-stimulated slices from control mice; however, p75-flox mice showed the same levels of co-localization in both conditions (Figure 3B). While the increase of endocytic proBDNF in glial cells appears to be modest when confronted with the whole cell volume, the same increase is considerably high taking into account that proBDNF is predominantly regionalized in the cell periphery.

Subcellular localization of proBDNF in glial cells was further resolved in super-resolution using 3D structured illumination microscopy (3D-SIM) (Figure 3D). In the cell body, proBDNF/GFP signal shows a clear vesicular pattern reminiscent of endocytic vesicles (Bergami et al., 2008), whereas in the cell periphery, most of the signal was punctate and distributed at astrocyte endfeet. Typically, astrocytes are highly branched cells with many small protrusions that contact the synaptic cleft (Reichenbach et al., 2010). Given the nanometer scale resolution of the 3D-SIM (115 nm x-y), our data suggest a synaptic localization of the neurotrophin.

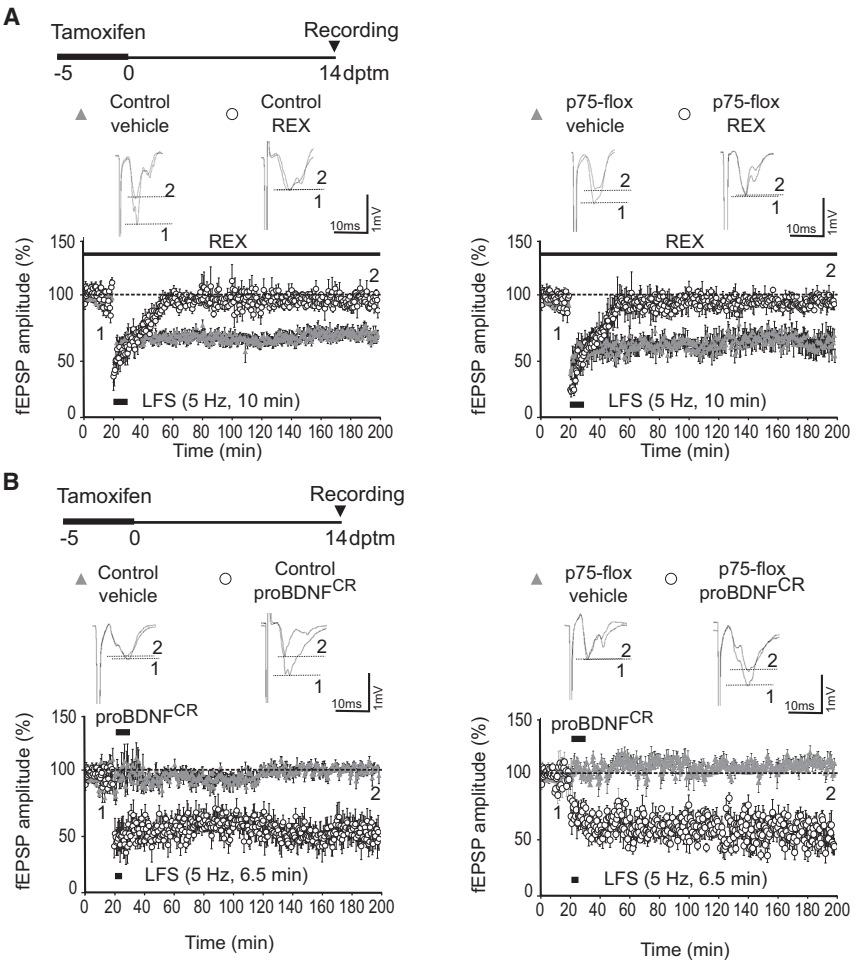

Figure 2. Glial p75^{NTR} Is Dispensable for LTD

(A) Schematic diagram shows the experimental paradigm used for tamoxifen treatment (−5 to 0 days) in p75-flox mice and control littermates. The histograms depict LTD evoked in the absence (vehicle) or presence (REX) of function-blocking p75^{NTR} antibody before, during, and after LFS (5 Hz, 10 min) in slices from control (left) and p75-flox (right) mice. Each point in the graphs shows the average fEPSP amplitude elicited in response to a test stimulus before (0–20 min), during (20–30), and after (30–200 min) LFS stimulation. The representative fEPSP traces recorded 10 min before (1) and 170 min after (2) LFS are shown on the top (control vehicle, 68.30% ± 3.71% and control REX, 97.28% ± 1.99% fEPSP 170 min from LFS; data are mean ± SEM; control vehicle, n = 14 slices, 8 mice; control REX, n = 12 slices, 6 mice; unpaired t test, $p < 0.0001$; and p75-flox vehicle, 53.42% ± 5.61% and p75-flox REX, 96.77% ± 4.76% fEPSP 170 min from LFS; data are mean ± SEM; p75-flox vehicle, n = 7 slices, 4 mice; p75-flox REX, n = 6 slices, 3 mice; unpaired t test, $p < 0.0001$).

(B) Schematic diagram shows the experimental paradigm as in (A). The histograms depict LTD evoked by LFS (5 Hz, 6.5 min) in the absence (vehicle) or presence of cleavage-resistant proBDNF (proBDNF^{CR}) in slices from control (left) and p75-flox (right) mice. Each point in the graphs shows the average fEPSP amplitude elicited in response to a test stimulus before (0–20 min), during (20–26.5 min), and after (26.5–200 min) LFS stimulation. The representative fEPSP traces recorded 10 min before (1) and 173.5 min after (2) LFS are shown on the top (control vehicle, 101.81% ± 6.89% and control proBDNF^{CR}, 48.70% ± 9.42% fEPSP 173.5 min from LFS; data are mean ± SEM; control vehicle, n = 9 slices, 5 mice; control proBDNF^{CR}, n = 6 slices, 3 mice; unpaired t test, $p = 0.0004$; and p75-flox vehicle, 112.07% ± 3.67% and p75-flox proBDNF^{CR}, 41.90% ± 6.84% fEPSP 173.5 min from LFS; data are mean ± SEM; p75-flox vehicle, n = 6 slices, 3 mice; p75-flox proBDNF^{CR}, n = 6 slices, 3 mice; unpaired t test, $p < 0.0001$).

To explore this possibility, ultra-thin sections were examined by transmission electron microscopy in pre-embedding experiments upon immunogold labeling with α-proBDNF or α-BDNF (Dieni et al., 2012). In sections from non-stimulated slices, gold particles were primarily seen in vesicular structures at pre-synaptic terminals (75% ± 7% pre-synaptic, 8% ± 2% post-synaptic, and 17% ± 3% astrocytic; or 68% ± 9% pre-synaptic, 18% ± 3% post-synaptic, and 14% ± 6% astrocytic of the total gold particle detected using α-proBDNF or α-BDNF, respectively), typically displaying clouds of synaptic vesicles proximal to post-synaptic density structures (Figure 4A). Following TBS, gold particles maintained their pre-synaptic localization, but were also clearly found in postsynaptic terminals and glial cells closely interacting with these synaptic complexes (34% ± 7% pre-synaptic, 20% ± 7% post-synaptic, and 46% ± 8% astrocytic; or 35% ± 7% pre-synaptic, 29% ± 3% post-synaptic, and 36% ± 4% astrocytic of the total gold particle detected using α-proBDNF or α-BDNF, respectively). While proBDNF in postsynaptic sites might be acquired from many different sources (i.e., local synthesis, synaptic transport, or internalization), its increase in glial cells (non-stimulated versus TBS-stimulated, unpaired t test, $p = 0.0374$ or $p = 0.0189$ using α-proBDNF or α-BDNF, respectively) implies that the neurotrophin is transferred from axon terminals to the neighboring glia. Accordingly, gold particles observed in stimulated slices appear contained in vesicle-like structures in proximity of the pre-synaptic membrane and contacting glia (Figure 4B). Most immunogold particles in glial cells (38% or 48% of the total gold particles detected in astrocytes using α-proBDNF or α-BDNF, respectively) were localized at peri-synaptic sites in a membrane-delimited area of 230 nm radius surrounding synaptic contacts (Figure 4A). At 70,000- to 100,000-fold magnification, immunogold labeling with both antibodies of this area revealed a subset of distinct aggregates of gold grains and, sporadically, single gold particles in vesicular structures (Figures 4B and 4C). We conclude that a significant pool of proBDNF-containing endocytic vesicles is created at peri-synaptic glia in response to TBS.

Uptake and Recycling of proBDNF

To obtain further insight into the intracellular storage and sorting of endocytic vesicles containing proBDNF/p75^{NTR} in astrocytes,

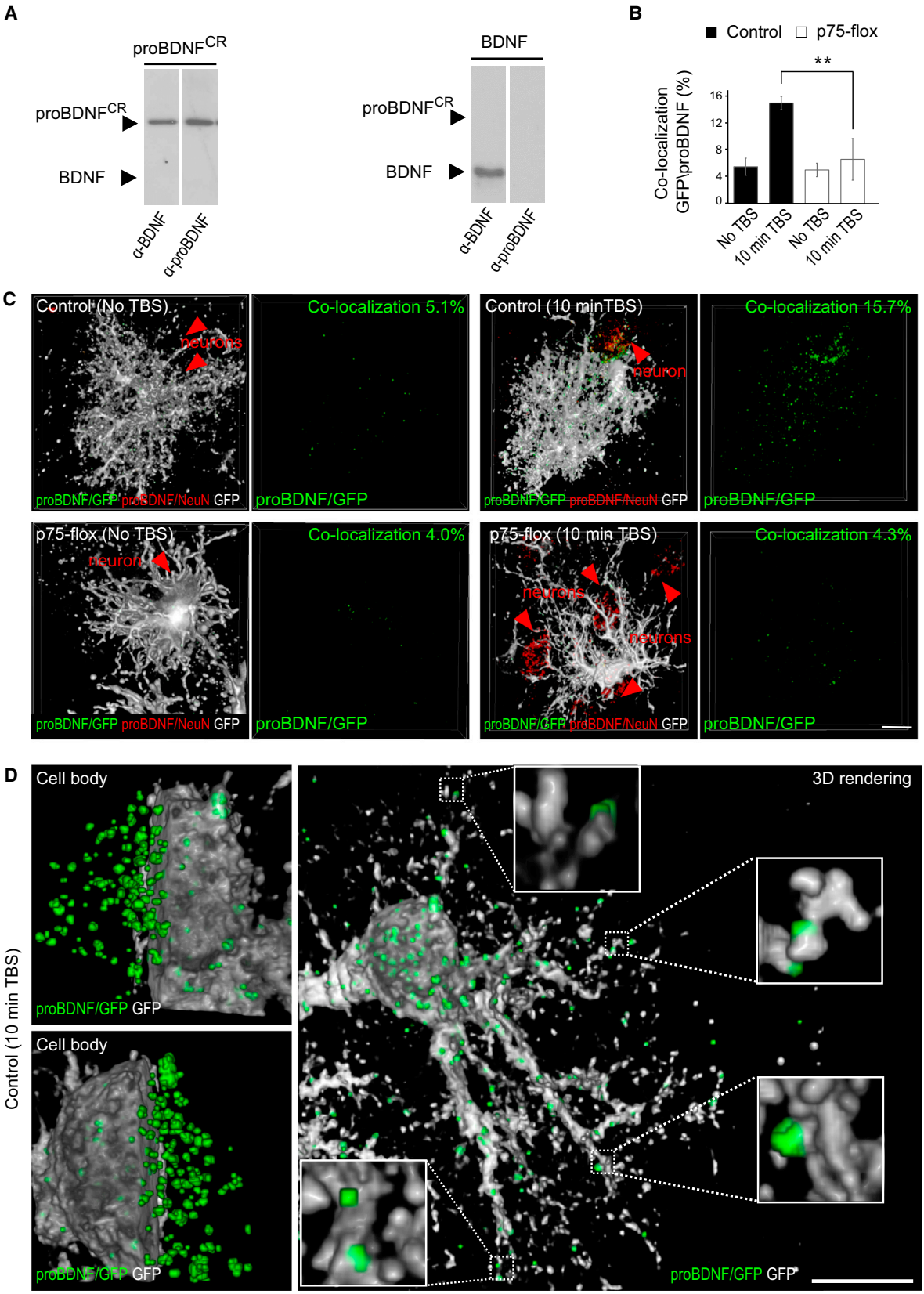

(legend on next page)

total internal reflection fluorescence (TIRF) microscopy was used to track single vesicles in real time. Cultured cortical astrocytes were transfected with $p75^{NTR}$ tagged with GFP (p75-GFP) for evanescent light excitation of p75-GFP residing within or in close proximity to the plasma membrane. Cells were exposed to proBDNF immunocomplexed with quantum dots (proBDNF-QDs) (Bergami et al., 2008) displaying the appearance of endocitic vesicles containing p75-GFP/proBDNF-QD complexes (Figures 5A–5F). Endocytic vesicles in juxtamembrane regions of the astrocyte showed a number of dynamic events: vesicles in active motion are confined at the site of internalization (Figure 5A) in thin (Figure 5B) or large (Figure 5C) membrane protrusions; alternatively, vesicles are transported for a short distance (Figure 5D). Thus, endocytic vesicles show limited trafficking and tend to localize at cell membrane margins delimiting the astrocyte endfeet. Moreover, we observed individual endocytic vesicles fusing each other into a larger vesicle (Figure 5E), which is in line with the presence of proBDNF aggregates observed by electron microscopy.

Next, we investigated whether endocytic vesicles containing p75-GFP/proBDNF-QD complex can eventually be recycled for exocytic fusion. Challenging astrocytes with glutamate (500 μM) disclosed proBDNF-QD release (Figure 5F). Only when p75-GFP fluorescence, which is normally concentrated at the site of proBDNF-QDs displaying orange fluorescence, vanishes and the proBDNF-QDs gain their original red fluorescence is it considered an exocytic event. Thus, endocytic vesicles containing $p75^{NTR}$/proBDNF represent the main storage compartment for the neurotrophin before routing to the secretory pathway.

Peri-Synaptic Glia Recycles BDNF for Neuronal TrkB Activation and LTP Maintenance

Functional implication for proBDNF glial recycling is that glial cells can release the neurotrophin in response to TBS, which fulfills the function to mediate the switch from early to late-phase LTP. To address this cellular property, we injected p75-flox mice with a lentivirus-transducing proBDNF (LV-$proBDNF^{stop}$) selectively in glial cells. We speculated that an ectopic source of proBDNF in $p75^{NTR}$-deficient astrocytes could replenish endocytic proBDNF and compensate for the lack of recycling in these cells, thereby restoring late-phase LTP deficits (Figure 6A). Pre-requisite for this mechanism is the evidence that in cultured astrocytes, endocytic and newly synthesized proBDNF are comparably secreted (Figure S6). In agreement with our hypothesis, we found that glial expression of proBDNF led to a complete rescue of the late-phase LTP, whereas mice injected in the contralateral hemisphere with control LV-GFP^{stop} virus showed no effect (Figures 6B and S2H). LV-$proBDNF^{stop}$ rescued the late-phase LTP deficit also when elicited by REX antibody in slices from control mice (Figure S7A). Thus, supplying glial cells with ectopic proBDNF compensates for the physiological requirement of neurotrophin recycling.

Given that mature BDNF, and not proBDNF, is well documented to act as an LTP mediator (Pang et al., 2004; Yang et al., 2014), we predict that transduced proBDNF undergoes intracellular or extracellular conversion to mature neurotrophin in order to restore the late-phase LTP. Our hypothesis was confirmed by injecting lentivirus-transducing cleavage-resistant $proBDNF^{CR}$ (LV-$proBDNF^{CRstop}$). In slices from p75-flox mice (Figures 6C and S2I) or control mice treated with REX (Figure S7A), $proBDNF^{CR}$ sourced by astrocytes could not produce a rescue of the phenotype. Our data indicate that processing of proBDNF sourced by glia is required for LTP maintenance and suggest a mechanistic link between proBDNF clearing and subsequent recycling as mature neurotrophin in response to synaptic potentiation.

To demonstrate that mature BDNF is sufficient for this effect, slices from p75-flox mice were perfused with BDNF (100 ng/mL) for 10 min following TBS. Exogenous application of the neurotrophin restored the late-phase LTP deficit induced by $p75^{NTR}$ deletion (Figures 6D and S2L) or inhibition by REX (Figure S7B). In contrast, application of $proBDNF^{CR}$ (100 ng/mL) failed to restore the late-phase LTP deficits in both conditions (Figures 6D and S7B). While we cannot exclude that other factors triggered by $p75^{NTR}$ may exist and play a role in LTP maintenance, these are not essential to mediate the late-phase LTP, as we demonstrated for BDNF. Finally, we showed that mature BDNF applied between 20 and 60 min after TBS was ineffective (Figures 6D and S2M), indicating that BDNF is required for a limited time window to sustain LTP and that glial recycling is sufficient to satisfy this temporal requirement.

Glial recycling and processing of proBDNF would result in highly localized activation of TrkB receptors on adjacent neurons. To assess this issue, we examined the phosphorylated TrkB (p-TrkB) profile at different time points after TBS in cortical slices from p75-flox mice and control littermates (Figure 7C) by using α-p-TrkB specific antibody (Figure S8A). Pre-requisite for this analysis is the evidence that in control slices, p-TrkB is virtually absent from glial cells (4.8% p-TrkB/GFP co-localization) (Figure 7A), which we have shown to lack the full-length TrkB receptor (Bergami et al., 2008). p-TrkB signal is instead restricted

Figure 3. Subcellular Localization of proBDNF in Glial Cells

(A) Western blotting depicts α-proBDNF and α-BDNF antibodies selectivity recognizing recombinant $proBDNF^{CR}$ and BDNF isoforms.

(B) Histogram depicts quantification of proBDNF/GFP co-localization in non-stimulated and TBS (10 min)-stimulated slices from p75-flox mice and control littermates (control No TBS, n = 10 cells, 4 slices, and 3 mice; control 10 min TBS, n = 13 cells, 4 slices, and 3 mice; p75-flox No TBS, n = 9 cells, 4 slices, and 3 mice; p75-flox 10 min TBS, n = 10 cells, 4 slices, and 3 mice; data are means ± SEM; unpaired t test, p = 0.0081; statistical significance $^{**}p < 0.01$).

(C) Three-dimensional reconstruction of GFP-positive astrocytes contacting neurons in non-stimulated and TBS (10 min)-stimulated slices from p75-flox mice and control littermates 14 dptm. The GFP signal is superimposed with proBDNF/GFP co-localizations. NeuN/GFP co-localizations are also shown. The quantification and distribution pattern of proBDNF/GFP signals are shown. The scale bar represents 10 μm.

(D) 3D-SIM images depict an astrocyte transduced with GFP in TBS (10 min) slice from control mice. The insets show 6× magnification of glial endfeet expressing proBDNF/GFP co-localization. The co-localization signal in the half-left (upper) or half-right (lower) part of the cell body is shown in 2× magnification images. The scale bar represents 10 μm.

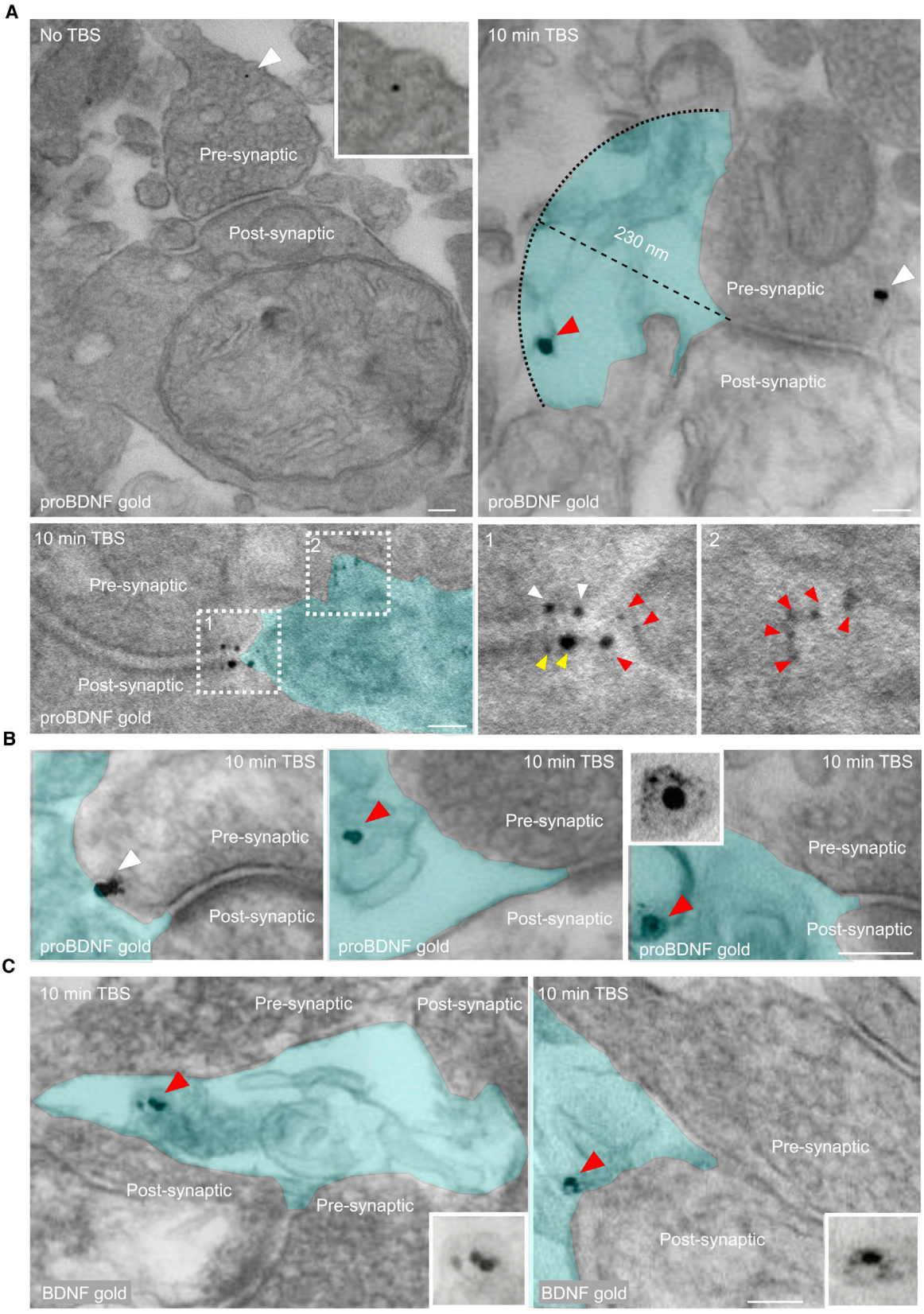

(legend on next page)

to neurons (97.6% p-TrkB/NeuN co-localization) (Figure 7A), often in close apposition to astrocyte endfeet (Figure 7B). Given that p-TrkB is essentially a fraction of the total receptor levels, we measured in a quantitative analysis that TrkB co-localizes with p-TrkB immunoreactivity at the stimulated areas (Figures S8B and S8C). For each experiment, p-TrkB/TrkB co-localization was normalized against the control condition in which slices were not stimulated. In control mice, we found that the p-TrkB/TrkB co-localization signal was significantly increased between 5 and 20 min from TBS and slowly returned to baseline after 60 min (Figure 7C). As a comparison, we measured the co-localization profile in stimulated slices from p75-flox mice. While the overall pattern of co-localization was similar between genotypes, the levels of co-localization in p75-flox mice were significantly reduced (Figure 7C). A decrease in p-TrkB/TrkB co-localization levels was most notable at 5 min following TBS and returned to control levels after 20 min. Remarkably, we obtained a complete rescue of the p-TrkB deficit by injecting p75-flox mice with LV-proBDNF^{stop}, but not with LV-proBDNF^{CRstop} (Figure 7D). Thus, proBDNF glial recycling and processing into the mature neurotrophin are required for tight temporal, spatial-, and stimulus-dependent TrkB phosphorylation on adjacent neurons.

BDNF Glial Recycling Is Essential for Visual Recognition Memory

There is significant evidence that the perirhinal cortex plays an essential role in familiarity-based object recognition (Brown and Aggleton, 2001; Murray et al., 2007), and that LTP in this brain area is implicated in visual recognition memory consolidation (Barker et al., 2006; Warburton et al., 2003). To assess whether glial recycling of proBDNF is involved in recognition memory consolidation in vivo, we subjected p75-flox mice and control littermates to an object recognition task (ORT). Mice performed the ORT with a retention interval between the sample phase and the test phase of 1 hr and 24 hr (Figure 8A). At 1 hr retention time, we found that p75-flox and control mice showed the expected preferential exploration of the novel object (Figure 8B). At 24 hr retention time, only control mice could discriminate familiar from novel objects, while p75-flox mice spent comparable time exploring both objects (Figure 8B). As a result, the discrimination index at 24 hr retention time was significantly lower in p75-flox mice compared to control littermates (Figure 8D). Thus, glial p75^{NTR} expression is required for memory consolidation.

Next, we tested whether rescuing proBDNF in glial cells could reverse the memory defect exhibited by p75-flox mice. We injected LV-proBDNF^{stop} into perirhinal cortex the last day of tamoxifen treatment and performed the ORT after 14 days. This latency ensures the complete recovery of the animals after surgery. Following the injection, mice fully recovered from the memory impairment discriminated between familiar and novel objects at 24 hr retention time (Figures 8C and 8D). Altogether, our behavioral data underline the physiological role of glial cells in BDNF-dependent recognition memory consolidation.

DISCUSSION

Regulation of endogenous BDNF secretion plays a critical role in perirhinal cortex LTP and LTD (Aicardi et al., 2004). The way in which BDNF availability is orchestrated and contributes to these forms of synaptic plasticity remains elusive, however. In the present work, we have investigated the interrelationship between neurons and astrocytes in governing BDNF trafficking during cortical plasticity. Major findings of the present study are that astrocytes can uptake proBDNF and recycle it as the mature neurotrophin, in a process essential to LTP maintenance and memory retention.

BDNF Glial Recycling in Cortical Plasticity

A key effector of this process is glial p75^{NTR}, which shows an unanticipated role in synaptic plasticity, stabilizing cortical LTP. By using conditional transgenic mice, we demonstrated that selective deletion of p75^{NTR} in glial cells virtually abolishes (Figure 1A) the late-phase LTP without affecting LTD (Figure 2A). Further, this significant deficit is fully rescued by p75^{NTR} re-expression (Figure 1C). This is in marked contrast to the conventional view that p75^{NTR} is uniquely involved in LTD (Lu et al., 2005; Rösch et al., 2005; Woo et al., 2005; Yang et al., 2014). Our data also show that glial p75^{NTR} regulates LTP by initiating proBDNF uptake and recycling, thereby governing activity-dependent release of the neurotrophin required for LTP maintenance. Clearly dependent on an initial supply of neuron-released proBDNF (Bergami et al., 2008), recycling may endow astrocytes with the ability to release previously internalized neurotrophins according to the synaptic need. When cortical astrocytes are devoid of p75^{NTR}, as in p75-flox mice, we sequentially observed that (1) proBDNF internalization in glial cells is prevented (Figures 3B and 3C), (2) TrkB phosphorylation in neighboring neurons is reduced (Figure 7C), and (3) the late-phase LTP is abolished (Figure 1A). Neither TrkB phosphorylation (Boutilier et al., 2008) nor the late-phase LTP (Rösch et al., 2005; Woo et al., 2005; Yang et al., 2014) is directly regulated by proBDNF, implying that conversion of the proBDNF to mature neurotrophin is occurring through the recycling process. To fully establish this causal link, we demonstrated that proBDNF expression in p75^{NTR}-deficient astrocytes compensates for the physiological requirement of glial recycling restoring both p-TrkB (Figure 7D) and LTP deficits (Figure 6B). On the contrary, a cleavage-resistant form of

Figure 4. Ultra-Structural Localization of proBDNF

(A) Electron microscopy images depict proBDNF-gold at pre-synaptic (white arrowheads) or post-synaptic (yellow arrowheads) terminals, or peri-synaptic (red arrowhead) astrocytes in sections from non-stimulated and TBS (10 min)-stimulated slices. The insets show 3× magnification of gold particles. An area of 230 nm radius surrounding a synaptic contact is highlighted (light blue).

(B) Localization of proBDNF-gold at pre-synaptic membrane (white arrowhead) and peri-synaptic glia (red arrowheads). The inset shows 4× magnification of gold particles in a vesicle-like structure.

(C) Electron microscopy images depict BDNF-gold (red arrowheads) at peri-synaptic glia. The insets show 3× magnification of gold particles in vesicle-like structures. The scale bars represent 50 nm.

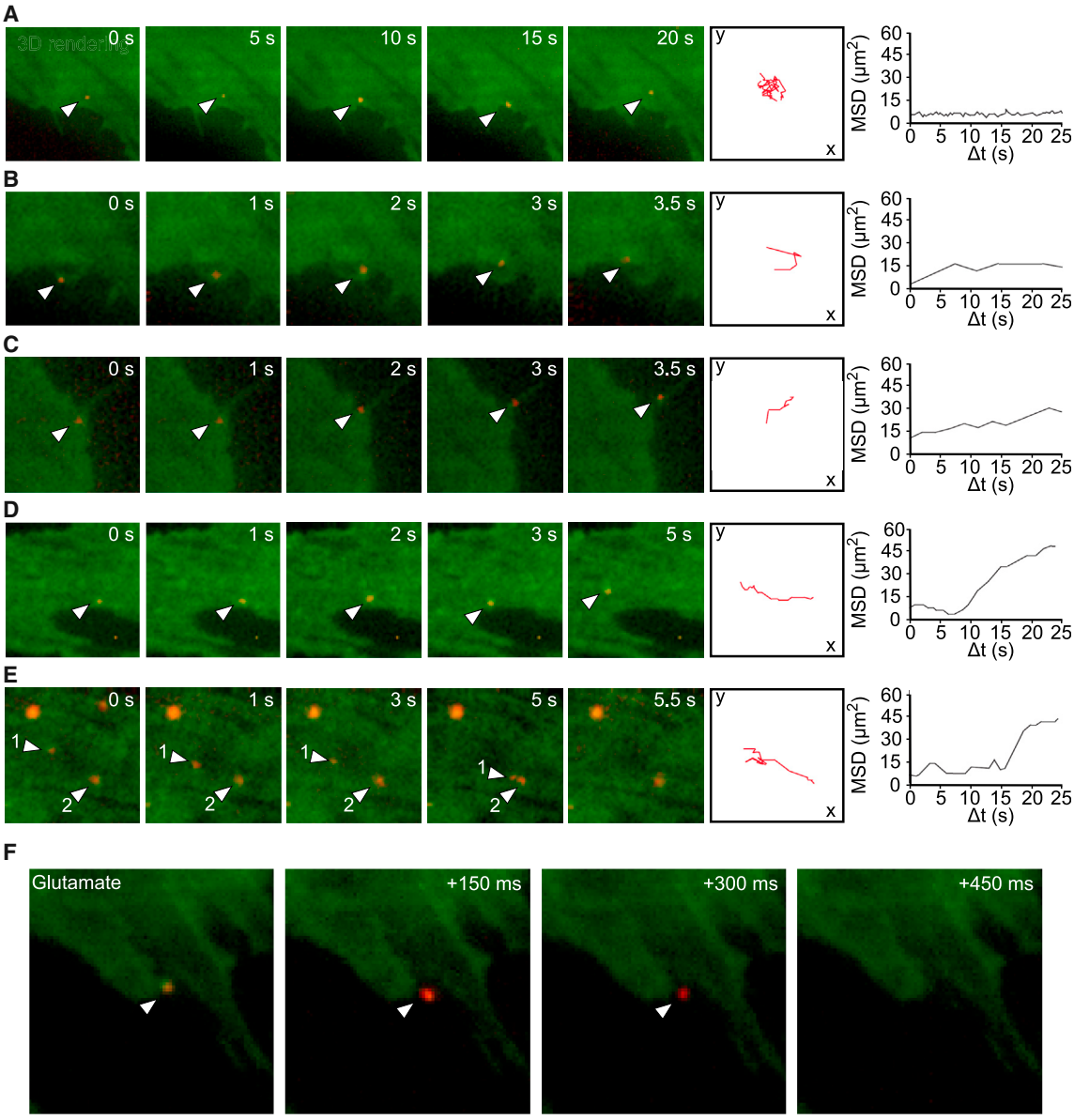

Figure 5. Sorting and Recycling of Endocytic proBDNF in Cultured Astrocytes

(A) TIRF images depict cultured astrocyte expressing p75-GFP treated with proBDNF-QDs. The time sequence of an endocytic vesicle containing p75-GFP/proBDNF-QDs (white arrowheads) residing at the site of internalization is shown; the image on the right depicts 2D (x-y) tracking of the vesicle, and the histogram shows vesicle motion by mean square displacement (MSD) analysis.

(B) Endocytic vesicle, as in (A), constrained in a thin glial protrusion.

(C) Endocytic vesicle, as in (A), constrained in a large glial protrusion.

(D) Endocytic vesicle, as in (A), moving for a short distance at the cell membrane margin.

(E) Two endocytic vesicles, as in (A), fusing each other; tracking and MSD analysis refer to vesicle number 1.

(F) Endocytic vesicle, as in (A), showing exocytic fusion: when p75-GFP/proBDNF-QD signal (orange-fluorescence) vanishes, proBDNF-QDs appear in their original red fluorescence (+150–300 ms) and finally disappear (+450 ms).

proBDNF showed no effect (Figure 6B). Where proBDNF conversion takes place remains to be established, and direct evaluation of the conversion sites remains an experimentally challenging problem. We favor that it may be achieved on a rapid timescale within the same vesicles that regulate recycling (Boutilier et al., 2008). However, we cannot exclude that proBDNF processing may occur in the extracellular space following its secretion from astrocytes and concomitant release of tPa from neurons (Pang et al., 2004) and astrocytes (Cassé et al., 2012). The latter, indeed, take up neuron-derived tPA and are able to re-release tPA in a regulated manner. Thus, glial recycling provides a mechanism for controlling synaptic clearing of proBDNF and

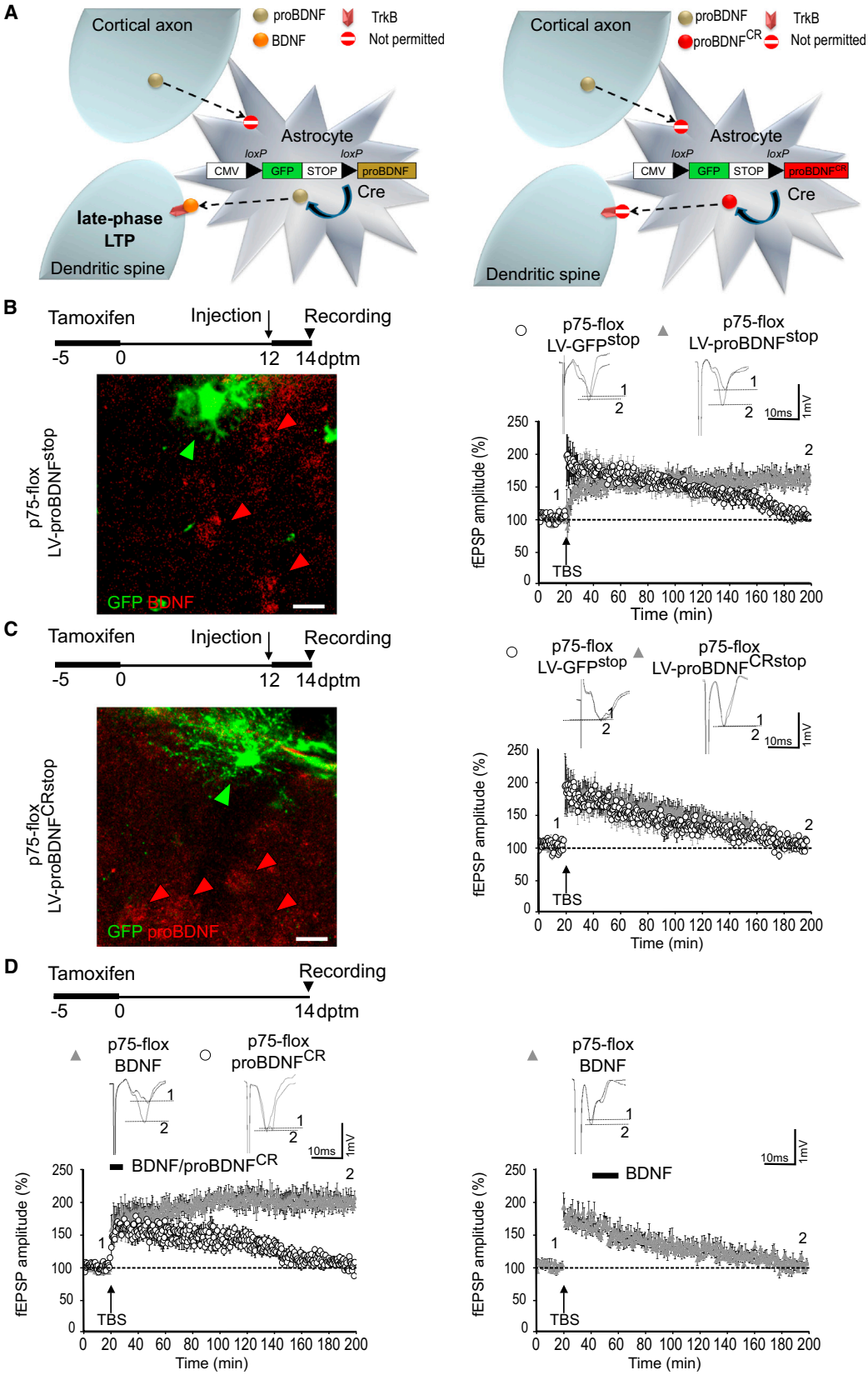

(legend on next page)

activation of TrkB receptors on adjacent neurons, thereby sustaining LTP.

Required Time Window for BDNF Recycling in LTP Maintenance

Glial recycling occurs in tight temporal conjunction with the LTP-inducing electrical stimulation. In slices from p75-flox mice, TrkB phosphorylation decreases rapidly following TBS and recovers 10 min later (Figure 7C). This interval represents the predicted time required for BDNF recycling by astrocytes. Our findings are in accordance with previous investigations showing that this time window is critical for BDNF action on LTP maintenance (Aicardi et al., 2004; Chen et al., 1999; Rex et al., 2007). Following from this evidence, we demonstrated that exogenous BDNF rescues the late-phase LTP deficit in slices from p75-flox mice only if applied for 10 min from TBS (Figure 6D), and, indeed, later administrations of exogenous BDNF failed to restore LTP maintenance. Thus, a time-sensitive increase in BDNF availability can compensate the physiological requirement for glial recycling. Additionally, recycling is required to sustain the size of the activity-dependent releasable pool of functional BDNF in this cortical area. This is in accordance with our previous findings that critical levels of endogenous BDNF released for 8–12 min after TBS are required for LTP maintenance in perirhinal cortex (Aicardi et al., 2004).

Different phases of LTP are sensitive to BDNF signaling in different circuits (Bramham and Messaoudi, 2005; Edelmann et al., 2014; Park and Poo, 2013). Previous investigations in hippocampus demonstrated that longer time windows are required for BDNF action on LTP maintenance. Late TBS-LTP in the CA1 region is prevented when TrkB phosphorylation was blocked by NMPP1 from 1 to 40 min post-TBS, but is not affected thereafter (Lu et al., 2011). Moreover, high-frequency stimulation (HFS)-induced LTP in the CA1 of hippocampal slices can be inhibited by TrkB-Fc from 30 to 60 min, but not from 70 to 100 min, after LTP induction (Kang et al., 1997). Even longer periods of BDNF action (about 8 hr) are necessary in dentate gyrus (Panja et al., 2014). Whether BDNF glial recycling and, to a larger extent, gliotransmission differently contribute to the duration of BDNF-TrkB signaling and LTP maintenance in individual circuits is presently not known. Further investigations will be necessary to correlate BDNF glial recycling and the requirement of BDNF in this possible diversity.

The activity dependence of glial recycling is also important from a functional point of view: it can ensure that BDNF recycled by glial cells is recruited by the same patterns of neuronal activity. BDNF recycled by glia may, then, synergistically regulate synaptic modifications according to synaptic needs. This might be particularly important for LTP maintenance, which requires threshold BDNF levels (Korte et al., 1995, 1996; Patterson et al., 1996). Neurons themselves can provide activity-dependent BDNF recycling via TrkB, and the endocytosed BDNF is fed back to the activity-dependent releasable pool required for LTP maintenance in the hippocampus (Santi et al., 2006; Wong et al., 2015). Endocytosed TrkB can also rapidly recycle to the membrane to promote sustained ERK signaling (Nagappan and Lu, 2005), and TrkB activation is known to stimulate BDNF release (Canossa et al., 1997). Thus, BDNF recycling by neurons and astrocytes provides a mechanism for increasing BDNF action with tight temporal, size-, and stimulus-specific expression and contributes to the consolidation of BDNF-induced synaptic changes.

Peri-Synaptic Storage of Endocytic Vesicles Containing proBDNF

Live imaging experiments using TIRF microscopy in cultured astrocytes showed that newly formed endocytic vesicles containing proBDNF/p75^{NTR} are mostly confined at glial endfeet (Figures 5A–5C) and recycle rapidly upon stimulation, releasing the neurotrophin to the extracellular milieu (Figure 5F). Constrained intracellular trafficking and fast recycling of endocytic vesicles imply that proBDNF is internalized locally in astrocytes before routing to the secretory pathway and endocytic vesicles represent the main storage compartment for the recycled neurotrophin. Ultra-structural characterization shows proBDNF immunoreactivity within vesicle-like structures in glial cells contacting the synapses (Figure 4). While this represents only a static picture of the neurotrophin sub-cellular localization, the appearance of gold particles at peri-synaptic sites likely denotes that a pool of ready, releasable vesicles containing the neurotrophin is available at the synapse for the time required for synaptic potentiation. In this regard, it is of tremendous functional

Figure 6. Ectopic BDNF Expression in Glial Cells Restores LTP Deficit

(A) Schematic diagrams illustrate astrocytes from p75-flox mice transduced with LV-proBDNF^{stop} (left) or LV-proBDNF^{CRstop} (right). The subsequent relevant steps (dashed arrows) are shown: (1) genetic deletion of glial p75^{NTR} precludes proBDNF transfer from neurons to astrocytes, and (2) astrocytes transduced with LV-proBDNF^{stop} source mature BDNF that is capable of TrkB activation and long-lasting LTP. In contrast, astrocytes transduced with LV-proBDNF^{CRstop} produce cleavage-resistant proBDNF^{CR} that is incapable of TrkB activation.

(B) Schematic diagram shows the experimental paradigm used for tamoxifen treatment. Following the first tamoxifen treatment (−5 to 0 days), a second treatment was applied for 2 additional days (12 to 14 days) following the injection with LV-GFP^{stop} in one hemisphere and LV-proBDNF^{stop} in the contralateral hemisphere. A confocal image depicts partially (green arrowhead) and fully (red arrowheads) recombined astrocytes transduced with LV-proBDNF^{stop}. The histogram shows LTP evoked in slices from p75-flox mice injected with LV-GFP^{stop} or LV-proBDNF^{stop} (LV-GFP^{stop}, 106.58% ± 3.24% and LV-proBDNF^{stop}, 158.20% ± 6.93% fEPSP 180 min from TBS; data are mean ± SEM; LV-GFP^{stop}, n = 6 slices, 3 mice; LV-proBDNF^{stop}, n = 8 slices, 4 mice; unpaired t test, $p < 0.0001$). For lentivirus description, see Figure S3. The scale bar represents 10 μm.

(C) Experiments using LV-proBDNF^{CRstop} are reported as in (B) (LV-GFP^{stop}, 108.43% ± 5.47% and LV-proBDNF^{CRstop}, 100.20% ± 3.34% fEPSP 180 min from TBS; data are mean ± SEM; LV-GFP^{stop}, n = 6 slices, 3 mice; LV-proBDNF^{stop}, n = 6 slices, 4 mice; unpaired t test, $p = 0.2281$). The scale bar represents 10 μm.

(D) Schematic diagram shows the experimental paradigm used for tamoxifen treatment (−5 to 0 days) in p75-flox mice. The histograms depict LTP evoked in slices from p75-flox mice treated with recombinant BDNF or proBDNF^{CR} (0 to 10 min) (left) or BDNF (20 to 60 min) (right) after TBS stimulation (p75-flox BDNF [0 to 10 min], 207.26% ± 9.94% and p75-flox proBDNF^{CR}, 108.50% ± 2.57% fEPSP 180 min from TBS; data are mean ± SEM; p75- flox BDNF [0 to 10 min], n = 6 slices, 3 mice; p75-flox proBDNF^{CR}, n = 8 slices, 6 mice; unpaired t test, $p < 0.0001$; and p75-flox BDNF [20 to 60 min], 106.11% ± 4.20% fEPSP 180 min from TBS; data are mean ± SEM; p75-flox BDNF [20 to 60 min], n = 6 slices, 3 mice).

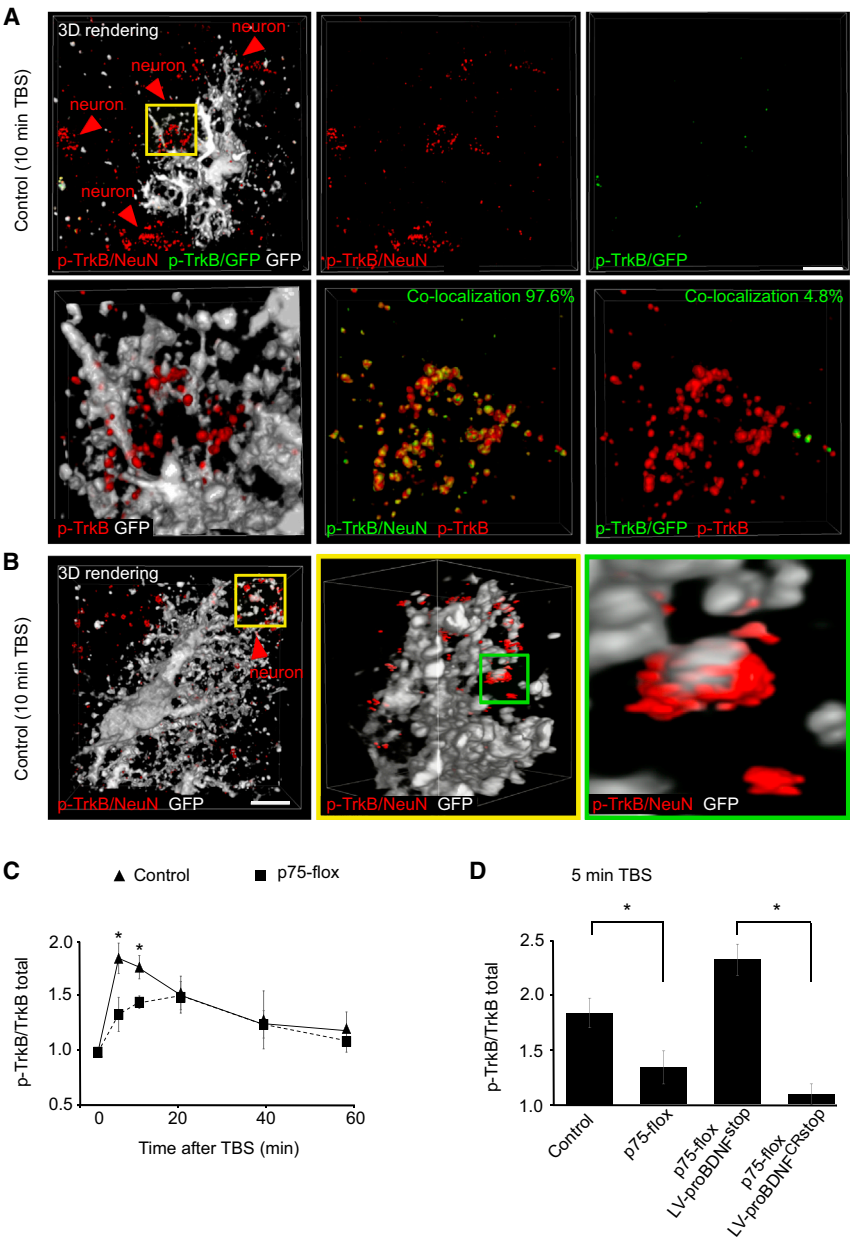

Figure 7. Glial Cells Recycle BDNF for TrkB Phosphorylation

(A) Left image shows 3D reconstruction of a GFP-positive astrocyte contacting NeuN-neurons from TBS (10 min)-stimulated slice in control mice. The GFP signal is superimposed with p-TrkB/NeuN and p-TrkB/GFP co-localizations. The distribution of p-TrkB/NeuN (middle) or p-TrkB/GFP (right) co-localizations is shown. The images below show 4× magnification of the region of interest (yellow box). In the same region, GFP (left), p-TrkB/NeuN (middle), and p-TrkB/GFP (right) are superimposed to p-TrkB signals. The scale bar represents 10 μm.

(B) Left image shows 3D reconstruction of a GFP-positive astrocyte contacting NeuN-neurons in TBS (10 min) slices from control mice. The GFP signal is superimposed with p-TrkB/NeuN co-localization. The middle image shows 4× magnification of the region of interest (yellow box). The right image shows 4× magnification of the region of interest (green box): p-TrkB/NeuN co-localization appear in close apposition to astrocyte endfeet. The scale bar represents 10 μm.

(C) Time course of p-TrkB/TrkB co-localization in p75-flox mice and control littermates (control; 0 min after TBS, n = 9 slices, 9 mice; 5 min after TBS, n = 8 slices, 8 mice; 10 min after TBS, n = 7 slices, 7 mice; 20 min after TBS, n = 9 slices, 9 mice; 40 min after TBS, n = 6 slices, 5 mice; 60 min after TBS, n = 6 slices, 5 mice; p75-flox; 0 min after TBS, n = 9 slices, 9 mice; 5 min after TBS, n = 7 slices, 7 mice; 10 min after TBS, n = 6 slices, 5 mice; 20 min after TBS, n = 9 slices, 9 mice; 40 min after TBS, n = 6 slices, 5 mice; 60 min after TBS, n = 6 slices, 5 mice. For methodological analysis, see Figure S5. The data are means ± SEM; unpaired t test, p [5 min after TBS] = 0.0371; p [10 min after TBS] = 0.0292; p [20 min after TBS] = 0.8576; p [40 min after TBS] = 0.8690; p [60 min after TBS] = 0.5554; statistical significance *p < 0.05).

(D) p-TrkB/TrkB co-localization signal in TBS (5 min)-stimulated slices from p75-flox mice and control littermates or p75-flox mice injected with LV-proBDNF^{stop} or LV-proBDNF^{CRstop} (control, n = 8 slices, 8 mice; p75-flox, n = 7 slices, 7 mice; p75-flox LV-BDNF^{stop}, n = 6 slices, 3 mice; p75-flox LV-BDNF^{CRstop}, n = 6 slices, 3 mice; data are means ± SEM; unpaired t test, p [control versus p75- flox] = 0.0371; p [p75-flox LV-BDNF^{stop} versus p75-flox LV-BDNF^{CRstop}] < 0.0001; statistical significance *p < 0.05).

relevance that highly localized activation of TrkB receptors in neurons was found in close apposition to astrocyte endfeet 10 min after stimulation (Figure 7B). At later times, the excess of endocytic proBDNF moves from glial cell periphery to the cell body (Bergami et al., 2008). Thus, sorting of endocytic vesicles leads to vesicle recycling and vesicle entering the degradation pathway, ending in a complete depletion of the neurotrophin.

Physiological Requirement of BDNF Glial Recycling in Memory Consolidation

In good correlation with a lack of LTP maintenance in the perirhinal cortex, p75-flox mice showed a behavioral deficit in the ORT (Figure 8B). Throughout the test phase of the ORT (Figure 8A), a novel object needs to be noticed and fixed in a memory trace, whereas the pre-existing memory trace of a familiar object needs to be re-loaded after a delay. Thus, ORT involves a higher memory load engaging long-term storage, recovery, and re-storage of the memory processing (Ennaceur, 2010), a mechanism that may require long-lasting synaptic potentiation. The time correlation between impaired LTP maintenance and recognition deficit of the familiar object after 24 hr in p75-flox mice supports the physiological relevance of BDNF glial recycling in memory retention. While ORT paradigm engages different brain structures, i.e., the hippocampus and nearby cortical areas including entorhinal and perirhinal cortex (Antunes and Biala, 2012), we

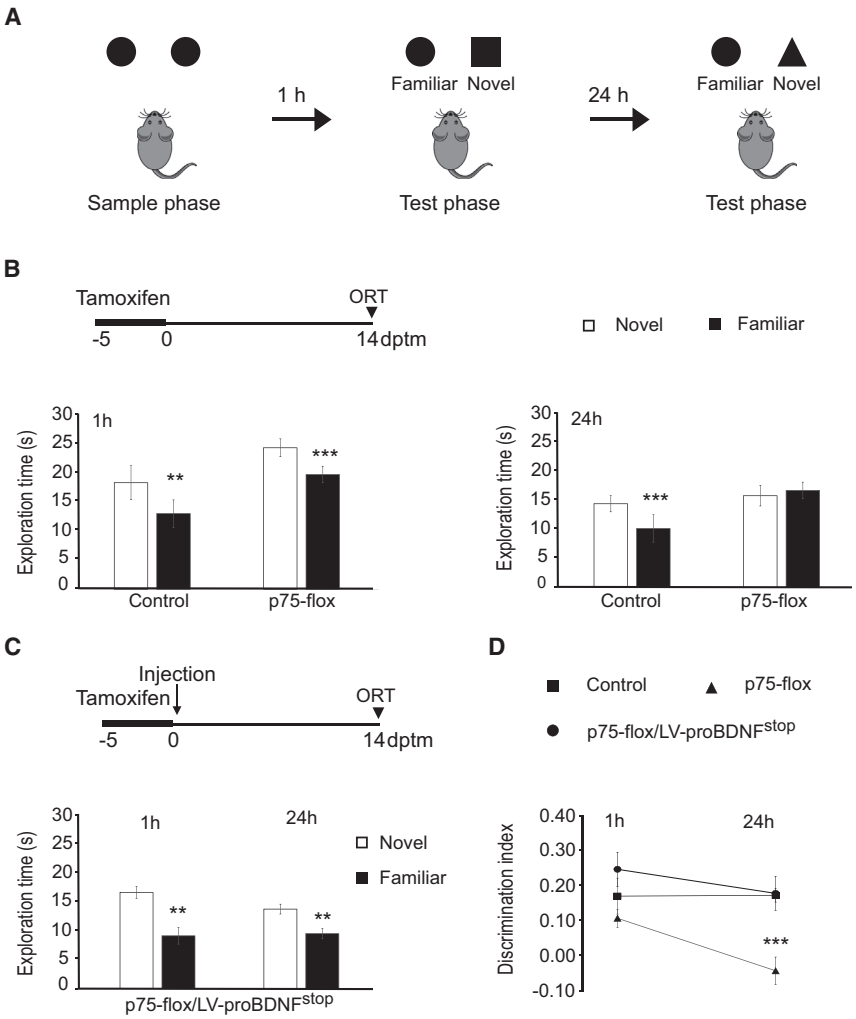

Figure 8. Recognition Memory Consolidation Requires BDNF Glial Recycling

(A) Schematic diagram depicts the experimental paradigm for ORT. The mice are exposed to two identical objects for one single sample phase of 5 min. After a delay of 1 and 24 hr, a test phase changing one familiar object with a novel object is performed.

(B) Schematic diagram shows the experimental paradigm used for tamoxifen treatment (−5 to 0 days) in p75-flox mice and control littermates. The histograms depict mean exploration time of the familiar object and of the novel object in the test phase for the 1 hr (left) and 24 hr (right) interval experiments (control, n = 8 mice; p75-flox, n = 10 mice; data are means ± SEM; paired t test; control 1 hr, p = 0.0069; p75-flox 1 hr, p = 0.0007; control 24 hr, p < 0.0001; p75-flox 24 hr, p = 0.4284; statistical significance **p < 0.01 and ***p < 0.001).

(C) Schematic diagram shows the experimental paradigm used for tamoxifen treatment (−5 to 0 days) in p75-flox mice injected with LV-proBDNF^{stop}. The histograms depict mean exploration time as in (B) (p75-flox LV-proBDNF^{stop}, n = 9 mice; data are means ± SEM; paired t test, p [1 hr] = 0.0100; p [24 hr] = 0.0052; statistical significance **p < 0.01).

(D) Discrimination index is plotted against time interval between familiarization and test phases in p75-flox mice, p75-flox mice injected with LV-proBDNF^{stop}, and control littermates (control, n = 8 mice; p75-flox, n = 10 mice; p75-flox LV-proBDNF^{stop}, n = 9 mice; data are means ± SEM; two-way ANOVA, time × genotype, post hoc Holm-Sidak method p [1 hr] = 0.223; p [24 hr] < 0.001; statistical significance ***p < 0.001).

demonstrated that proBDNF selectively expressed in glial cells from the perirhinal cortex is sufficient to restore long-term recognition memory (Figure 8C). This indicates that glial recycling in other medial temporal lobe structures possibly involved in recognition memory is not required to mediate the formation of a long-term recognition memory. A similar effect restricted to perirhinal cortex has been proved for ERK activation (Silingardi et al., 2011), a molecule downstream of BDNF signaling.

A striking correlation with our behavioral data is provided by the demonstration that transgenic mice expressing tetanus neurotoxin (TeNT) selectively in astrocytes were accompanied by impaired behavioral performance in the ORT (Lee et al., 2014). Sustained TeNT expression in astrocytes can be expected to inhibit the trafficking of all vesicles, including those responsible for BDNF recycling (Bergami et al., 2008). Whether glial TeNT expression prevents LTP maintenance in perirhinal cortex is presently not known; however, data from Lee et al. (2014) and our data suggest that among the entirety of neuroactive molecules secreted by glial cells, BDNF is the one requested for recognition memory. Our data therefore support BDNF as an essential gliotransmitter regulating synaptic plasticity.

EXPERIMENTAL PROCEDURES

Mice

Mouse lines are described in the Supplemental Experimental Procedures.

Antibodies

Antibodies are described in the Supplemental Experimental Procedures.

Viral Vectors

Viral vectors are described in the Supplemental Experimental Procedures.

Electrophysiological Recording

Slices from perirhinal cortex were prepared from p75-flox, control littermates, or wild-type mice (7–9 weeks old). The brain was removed and placed in cold (5°C) oxygenated (95% O_2 and 5% CO_2) artificial cerebrospinal fluid (ACSF) containing 124.0 mM NaCl, 4.4 mM KCl, 1 mM NaH_2PO_4, 2.5 mM $CaCl_2$, 1.3 mM $MgCl_2$, 26.2 mM $NaHCO_3$, 10 mM glucose, and 2 mM L-ascorbic acid (Sigma-Aldrich). Horizontal cortex slices (300 μm thick) were prepared using a vibratome and maintained in a chamber containing oxygenated ACSF at room temperature. After a minimum recovery period of at least 1 hr, a single slice was transferred into a submersion recording chamber perfused (3 mL/min) with oxygenated ACSF at 32°C ± 0.2°C and square current pulses (duration 0.2 ms) were applied every 30 s (0.033 Hz) using a stimulus generator (WPI, stimulus isolator A360) connected through a stimulus isolation unit to a

concentric bipolar electrode (40–80 KΩ, FHC) positioned in layers II/III on the temporal side of the rhinal sulcus. Evoked extracellular fEPSPs were recorded using an Axoclamp-2B amplifier (Axon Instruments) with ACSF-filled glass micropipette pulled on a vertical puller (Narishige PC-10, resistance [<5 MΩ]), inserted in layers II/III at around 500 μm from the stimulation electrode, and analyzed using Axoscope 8.0 software (Axon Instruments). Baseline responses were obtained every 30 s with a stimulus intensity adjusted to induce ≈50% of the maximal synaptic response. After 20 min of stable baseline, LTP was evoked by TBS (100 Hz; four sets of stimulations delivered 15 s apart, each one consisting of ten bursts of five pulses at 100 Hz with inter-burst intervals of 150 ms). LTD was evoked by LFS of either 3,000 stimuli (10 min) or 1,950 stimuli (6.5 min) at 5 Hz. fEPSPs were plotted as amplitude and slope and we selected only those showing similar trend. Each point represents the responses every 30 s expressed as means ± SEM. In some experiments, recombinant BDNF (100 ng/mL) or recombinant cleavage-resistant proBDNF (100 ng/mL) was added from 2 min before to 10 min after stimulation or from 20 to 40 min after TBS. In some experiments, cortical slices were incubated with REX antibody for at least 1 hr before recording and throughout all the recording time.

Immunostaining

Immunocytochemistry and immunohistochemistry are described in the Supplemental Experimental Procedures.

Stereotaxic Surgery

Stereotaxic surgery is described in the Supplemental Experimental Procedures.

Western Blot Experiments

Western blot experiments are described in the Supplemental Experimental Procedures.

Confocal Microscopy and Quantitative Image Analysis

Confocal microscopy experiments are described in the Supplemental Experimental Procedures.

3D-SIM

3D-SIM is described in the Supplemental Experimental Procedures.

Electron Microscopy

Electron microscopy is described in the Supplemental Experimental Procedures.

Object Recognition Test

ORT was performed in a Y-apparatus with high, homogenous white walls, 30 cm high: one arm was used as start arm and had a sliding door to control access to the arena; the other two arms were used to display the objects (Bartko et al., 2010; Leger et al., 2012). The start arm is 26 cm in length, with the sliding door placed at 13 cm, and the lateral arms are 18 cm. All arms are 10 cm wide. On the first day (habituation day) mice explored the arena for 20 min. The following day, the learning session (sample phase) was performed: animals were free to explore the arena for 5 min, which contained two identical objects, one for each arm, placed at the end of the arm. At 1 or 24 hr after the sample phase, the test phase was run, during which animals were free to explore the arena containing two objects, the familiar object and a novel one. Arena and objects were cleaned up between trials to stop the build-up of olfactory cues. The discrimination index was calculated as follows: (TNew − TOld)/(TNew + TOld), with TNew and TOld being the time spent exploring the new and the familiar objects, respectively. A video camera was mounted above the apparatus to record trials with the EthoVision software (Noldus). The exploration time was taken as the time during which mice approached the objects with muzzle and paws.

Statistical Analysis

All data were run for a normality test before a statistical comparison test. Data normally distributed were summarized by mean ± SEM. Comparison between two different groups was assessed by an unpaired t test or paired t test. For an ORT discrimination index, two-way ANOVA followed by a Holm-Sidak method test was used. The level of significance used was $p < 0.05$.

SUPPLEMENTAL INFORMATION

Supplemental Information includes Supplemental Experimental Procedures and eight figures and can be found with this article online at http://dx.doi.org/10.1016/j.neuron.2016.09.031.

AUTHOR CONTRIBUTIONS

B.V. participated in the experimental design, performed most of the experiments, and discussed the results; G.B. and B.V. performed electrophysiology; S.S. and B.V. designed and performed 3D-SIM and electron microscopy; R.B. designed and provided the lentiviruses and antibody specificity assessment; R.M. and N.B. designed and performed behavioral analysis; and M.C. conceived and supervised the experiments and prepared the manuscript and figures together with B.V.

ACKNOWLEDGMENTS

We acknowledge Corinna Giorgi for her critical reading of the manuscript, Massimo Gamberini for technical assistance, Ranzi Barbara for lab management, Moses Chao for providing p-TrkB and REX antibody, Brian A. Pierchala for providing $p75^{lox/lox}$ mice, Antonino Cattaneo for providing recombinant BDNF and $proBDNF^{CR}$, Magdalena Götz for providing GLAST-Cre ER^{T2} mice, and the IN-BDNF consortium for scientific support. Funding to M.C. was provided by PRIN 2012, 2016, and partial support from the Italian Research Council (Framework Agreement EBRI-CNR 2015-2017); funding to R.B. was provided by the Deutsche Forschungsgemeinschaft SFB-TRR58, A10, and BL567-3/2; and funding to S.S. was provided by Conto Capitale 2013-Ministero della Salute.

Received: April 5, 2016
Revised: July 24, 2016
Accepted: September 8, 2016
Published: October 13, 2016

REFERENCES

Aicardi, G., Argilli, E., Cappello, S., Santi, S., Riccio, M., Thoenen, H., and Canossa, M. (2004). Induction of long-term potentiation and depression is reflected by corresponding changes in secretion of endogenous brain-derived neurotrophic factor. Proc. Natl. Acad. Sci. USA *101*, 15788–15792.

Allen, N.J., and Barres, B.A. (2005). Signaling between glia and neurons: focus on synaptic plasticity. Curr. Opin. Neurobiol. *15*, 542–548.

Antunes, M., and Biala, G. (2012). The novel object recognition memory: neurobiology, test procedure, and its modifications. Cogn. Process. *13*, 93–110.

Araque, A., Carmignoto, G., Haydon, P.G., Oliet, S.H.R., Robitaille, R., and Volterra, A. (2014). Gliotransmitters travel in time and space. Neuron *81*, 728–739.

Barker, G.R.I., Warburton, E.C., Koder, T., Dolman, N.P., More, J.C.A., Aggleton, J.P., Bashir, Z.I., Auberson, Y.P., Jane, D.E., and Brown, M.W. (2006). The different effects on recognition memory of perirhinal kainate and NMDA glutamate receptor antagonism: implications for underlying plasticity mechanisms. J. Neurosci. *26*, 3561–3566.

Bartko, S.J., Cowell, R.A., Winters, B.D., Bussey, T.J., and Saksida, L.M. (2010). Heightened susceptibility to interference in an animal model of amnesia: impairment in encoding, storage, retrieval—or all three? Neuropsychologia *48*, 2987–2997.

Bergami, M., Santi, S., Formaggio, E., Cagnoli, C., Verderio, C., Blum, R., Berninger, B., Matteoli, M., and Canossa, M. (2008). Uptake and recycling of pro-BDNF for transmitter-induced secretion by cortical astrocytes. J. Cell Biol. *183*, 213–221.

Boutilier, J., Ceni, C., Pagdala, P.C., Forgie, A., Neet, K.E., and Barker, P.A. (2008). Proneurotrophins require endocytosis and intracellular proteolysis to induce TrkA activation. J. Biol. Chem. *283*, 12709–12716.

Bramham, C.R., and Messaoudi, E. (2005). BDNF function in adult synaptic plasticity: the synaptic consolidation hypothesis. Prog. Neurobiol. *76*, 99–125.

Brown, M.W., and Aggleton, J.P. (2001). Recognition memory: what are the roles of the perirhinal cortex and hippocampus? Nat. Rev. Neurosci. *2*, 51–61.

Canossa, M., Griesbeck, O., Berninger, B., Campana, G., Kolbeck, R., and Thoenen, H. (1997). Neurotrophin release by neurotrophins: implications for activity-dependent neuronal plasticity. Proc. Natl. Acad. Sci. USA *94*, 13279–13286.

Cassé, F., Bardou, I., Danglot, L., Briens, A., Montagne, A., Parcq, J., Alahari, A., Galli, T., Vivien, D., and Docagne, F. (2012). Glutamate controls tPA recycling by astrocytes, which in turn influences glutamatergic signals. J. Neurosci. *32*, 5186–5199.

Chen, G., Kolbeck, R., Barde, Y.A., Bonhoeffer, T., and Kossel, A. (1999). Relative contribution of endogenous neurotrophins in hippocampal long-term potentiation. J. Neurosci. *19*, 7983–7990.

Dieni, S., Matsumoto, T., Dekkers, M., Rauskolb, S., Ionescu, M.S., Deogracias, R., Gundelfinger, E.D., Kojima, M., Nestel, S., Frotscher, M., and Barde, Y.A. (2012). BDNF and its pro-peptide are stored in presynaptic dense core vesicles in brain neurons. J. Cell Biol. *196*, 775–788.

Edelmann, E., Lessmann, V., and Brigadski, T. (2014). Pre- and postsynaptic twists in BDNF secretion and action in synaptic plasticity. Neuropharmacology *76*, 610–627.

Ennaceur, A. (2010). One-trial object recognition in rats and mice: methodological and theoretical issues. Behav. Brain Res. *215*, 244–254.

Figurov, A., Pozzo-Miller, L.D., Olafsson, P., Wang, T., and Lu, B. (1996). Regulation of synaptic responses to high-frequency stimulation and LTP by neurotrophins in the hippocampus. Nature *381*, 706–709.

Greenberg, M.E., Xu, B., Lu, B., and Hempstead, B.L. (2009). New insights in the biology of BDNF synthesis and release: implications in CNS function. J. Neurosci. *29*, 12764–12767.

Halassa, M.M., and Haydon, P.G. (2010). Integrated brain circuits: astrocytic networks modulate neuronal activity and behavior. Annu. Rev. Physiol. *72*, 335–355.

Hempstead, B.L. (2015). Brain-derived neurotrophic factor: three ligands, many actions. Trans. Am. Clin. Climatol. Assoc. *126*, 9–19.

Kang, H., Welcher, A.A., Shelton, D., and Schuman, E.M. (1997). Neurotrophins and time: different roles for TrkB signaling in hippocampal long-term potentiation. Neuron *19*, 653–664.

Korte, M., Carroll, P., Wolf, E., Brem, G., Thoenen, H., and Bonhoeffer, T. (1995). Hippocampal long-term potentiation is impaired in mice lacking brain-derived neurotrophic factor. Proc. Natl. Acad. Sci. USA *92*, 8856–8860.

Korte, M., Staiger, V., Griesbeck, O., Thoenen, H., and Bonhoeffer, T. (1996). The involvement of brain-derived neurotrophic factor in hippocampal long-term potentiation revealed by gene targeting experiments. J. Physiol. Paris *90*, 157–164.

Lee, H.S., Ghetti, A., Pinto-Duarte, A., Wang, X., Dziewczapolski, G., Galimi, F., Huitron-Resendiz, S., Piña-Crespo, J.C., Roberts, A.J., Verma, I.M., et al. (2014). Astrocytes contribute to gamma oscillations and recognition memory. Proc. Natl. Acad. Sci. USA *111*, E3343–E3352.

Leger, M., Quiedeville, A., Paizanis, E., Natkunarajah, S., Freret, T., Boulouard, M., and Schumann-Bard, P. (2012). Environmental enrichment enhances episodic-like memory in association with a modified neuronal activation profile in adult mice. PLoS ONE *7*, e48043.

Lessmann, V., and Brigadski, T. (2009). Mechanisms, locations, and kinetics of synaptic BDNF secretion: an update. Neurosci. Res. *65*, 11–22.

Lu, B., Pang, P.T., and Woo, N.H. (2005). The yin and yang of neurotrophin action. Nat. Rev. Neurosci. *6*, 603–614.

Lu, Y., Ji, Y., Ganesan, S., Schloesser, R., Martinowich, K., Sun, M., Mei, F., Chao, M.V., and Lu, B. (2011). TrkB as a potential synaptic and behavioral tag. J. Neurosci. *31*, 11762–11771.

Mischel, P.S., Smith, S.G., Vining, E.R., Valletta, J.S., Mobley, W.C., and Reichardt, L.F. (2001). The extracellular domain of p75NTR is necessary to inhibit neurotrophin-3 signaling through TrkA. J. Biol. Chem. *276*, 11294–11301.

Murray, E.A., Bussey, T.J., and Saksida, L.M. (2007). Visual perception and memory: a new view of medial temporal lobe function in primates and rodents. Annu. Rev. Neurosci. *30*, 99–122.

Nagappan, G., and Lu, B. (2005). Activity-dependent modulation of the BDNF receptor TrkB: mechanisms and implications. Trends Neurosci. *28*, 464–471.

Pang, P.T., Teng, H.K., Zaitsev, E., Woo, N.T., Sakata, K., Zhen, S., Teng, K.K., Yung, W.-H., Hempstead, B.L., and Lu, B. (2004). Cleavage of proBDNF by tPA/plasmin is essential for long-term hippocampal plasticity. Science *306*, 487–491.

Panja, D., Kenney, J.W., D'Andrea, L., Zalfa, F., Vedeler, A., Wibrand, K., Fukunaga, R., Bagni, C., Proud, C.G., and Bramham, C.R. (2014). Two-stage translational control of dentate gyrus LTP consolidation is mediated by sustained BDNF-TrkB signaling to MNK. Cell Rep. *9*, 1430–1445.

Park, H., and Poo, M.M. (2013). Neurotrophin regulation of neural circuit development and function. Nat. Rev. Neurosci. *14*, 7–23.

Patterson, S.L., Abel, T., Deuel, T.A., Martin, K.C., Rose, J.C., and Kandel, E.R. (1996). Recombinant BDNF rescues deficits in basal synaptic transmission and hippocampal LTP in BDNF knockout mice. Neuron *16*, 1137–1145.

Reichenbach, A., Derouiche, A., and Kirchhoff, F. (2010). Morphology and dynamics of perisynaptic glia. Brain Res. Brain Res. Rev. *63*, 11–25.

Rex, C.S., Lin, C.-Y., Kramár, E.A., Chen, L.Y., Gall, C.M., and Lynch, G. (2007). Brain-derived neurotrophic factor promotes long-term potentiation-related cytoskeletal changes in adult hippocampus. J. Neurosci. *27*, 3017–3029.

Rösch, H., Schweigreiter, R., Bonhoeffer, T., Barde, Y.-A., and Korte, M. (2005). The neurotrophin receptor p75NTR modulates long-term depression and regulates the expression of AMPA receptor subunits in the hippocampus. Proc. Natl. Acad. Sci. USA *102*, 7362–7367.

Santi, S., Cappello, S., Riccio, M., Bergami, M., Aicardi, G., Schenk, U., Matteoli, M., and Canossa, M. (2006). Hippocampal neurons recycle BDNF for activity-dependent secretion and LTP maintenance. EMBO J. *25*, 4372–4380.

Silingardi, D., Angelucci, A., De Pasquale, R., Borsotti, M., Squitieri, G., Brambilla, R., Putignano, E., Pizzorusso, T., and Berardi, N. (2011). ERK pathway activation bidirectionally affects visual recognition memory and synaptic plasticity in the perirhinal cortex. Front. Behav. Neurosci. *5*, 84.

Sloan, S.A., and Barres, B.A. (2014). Looks can be deceiving: reconsidering the evidence for gliotransmission. Neuron *84*, 1112–1115.

Teng, H.K., Teng, K.K., Lee, R., Wright, S., Tevar, S., Almeida, R.D., Kermani, P., Torkin, R., Chen, Z.Y., Lee, F.S., et al. (2005). ProBDNF induces neuronal apoptosis via activation of a receptor complex of p75NTR and sortilin. J. Neurosci. *25*, 5455–5463.

Teng, K.K., Felice, S., Kim, T., and Hempstead, B.L. (2010). Understanding proneurotrophin actions: recent advances and challenges. Dev. Neurobiol. *70*, 350–359.

Warburton, E.C., Koder, T., Cho, K., Massey, P.V., Duguid, G., Barker, G.R.I., Aggleton, J.P., Bashir, Z.I., and Brown, M.W. (2003). Cholinergic neurotransmission is essential for perirhinal cortical plasticity and recognition memory. Neuron *38*, 987–996.

Wong, Y.-H., Lee, C.-M., Xie, W., Cui, B., and Poo, M.M. (2015). Activity-dependent BDNF release via endocytic pathways is regulated by synaptotagmin-6 and complexin. Proc. Natl. Acad. Sci. USA *112*, E4475–E4484.

Woo, N.H., Teng, H.K., Siao, C.-J., Chiaruttini, C., Pang, P.T., Milner, T.A., Hempstead, B.L., and Lu, B. (2005). Activation of p75NTR by proBDNF facilitates hippocampal long-term depression. Nat. Neurosci. *8*, 1069–1077.

Yang, J., Harte-Hargrove, L.C., Siao, C.J., Marinic, T., Clarke, R., Ma, Q., Jing, D., Lafrancois, J.J., Bath, K.G., Mark, W., et al. (2014). proBDNF negatively regulates neuronal remodeling, synaptic transmission, and synaptic plasticity in hippocampus. Cell Rep. *7*, 796–806.

Zuccaro, E., Bergami, M., Vignoli, B., Bony, G., Pierchala, B.A., Santi, S., Cancedda, L., and Canossa, M. (2014). Polarized expression of p75(NTR) specifies axons during development and adult neurogenesis. Cell Rep. *7*, 138–152.